Journal of Materials Science and Chemical Engineering, 2017, 5, 44-54
http://www.scirp.org/journal/msce
ISSN Online: 2327-6053
ISSN Print: 2327-6045

Electro-Chemical Impedance Spectral (EIS) Study of Patinated Bronze Corrosion in Sulfate Media: Experimental Design Approach

Aymen Chaabani[1,2], Safa Aouadi[1,2], Nébil Souissi[1], X. Ramón Nóvoa[3]

[1]Preparatory Institute For Engineering Studies El Manar, University of Tunis El Manar, Farhat Hached University Campus of El Manar, Tunisia
[2]Faculty of Sciences of Bizerte, University of Carthage, Jarzouna, Tunisia
[3]ENCOMAT Group, E.E.I., University of Vigo, Vigo, Spain
Email: aymen.chaab@gmail.com

How to cite this paper: Chaabani, A., Aouadi, S., Souissi, N. and Nóvoa, X.R. (2017) Electro-Chemical Impedance Spectral (EIS) Study of Patinated Bronze Corrosion in Sulfate Media: Experimental Design Approach. *Journal of Materials Science and Chemical Engineering*, **5**, 44-54.
https://doi.org/10.4236/msce.2017.510004

Received: September 25, 2017
Accepted: October 28, 2017
Published: October 31, 2017

Abstract

The aim of the present investigation was to model the experimental conditions of tin bronze patination using full factorial experimental design. In this sense, a full factorial design approach was developed to model the corrosion behavior of patinated tin bronze alloy in sulfate electrolyte. Three experimental factors (the immersion time in the chloride electrolyte, the potential limit for the anodic sweep Elim, and the potential scan rate) were chosen to identify the significant factor on the patina growth process at the bronze substrate. The experimental responses were the kinetic parameters extracted from the electro-chemical spectra (EIS) for eight different experiments. An equivalent electrical circuit containing an electrolyte resistance (Re), a double layer capacitance (CPE_{dl}), a charge transfer resistance (R_t) and Gerischer element (G), was developed to model the patinated bronze corrosion process. The electro-chemical spectra (EIS) show that the corrosion process of the patinated bronze alloy occurred from a chemical reaction is followed by an electrochemical one. Analysis of the experimental responses showed that while the scan rate is the most influent factor for the corrosion potential (E_{corr}), the electrolyte resistance (Re), and the double layer capacitance CPE_{dl} variation, the potential limit is the significant factor for charge transfer resistance Rt, reciprocal of the admittance parameter Y_0 and the effective transfer rate of the chemical reaction k variation.

Keywords

Bronze, Corrosion, Experimental Design, Electrochemical Impedance Spectroscopy, Gerischer Impedance

1. Introduction

Cu-Sn alloys were used since antiquity to produce sculptures, coins and artefacts. These materials exhibit good mechanical and esthetical properties.

Numerous analytical techniques were used to study tin bronze corrosion mechanisms [1] [2] [3]. Electrochemical investigations were also undertaken [4]-[8]. We used the cyclic voltammetry technique to explore archaeological Punic bronze corrosion behavior in chloride electrolyte [9] and we compared also modern and archaeological materials voltammetric behaviors [10] recently, we showed [11] that the bronze corrosion reaction order with respect to chloride ions varied as the halide content changed. In fact, for $[Cl^-] < 0.5$ M, the reaction order was about 0.22 suggesting that the Cu10Sn bronze alloy dissolution was not strongly dependent with Cl^- ions which could act as corrosion initiator. For $[Cl^-] > 0.5$ M the bronze mechanism alloy was controlled by copper oxidation. Two determining steps were evidenced where the cuprous chloride formation was followed by $CuCl_2^-$ complex.

We used also electro-chemical impedance spectroscopy to characterize the corrosion behavior of archaeological bronze in 0.1 M chloride medium interface. Indeed, a simple electrical equivalent circuit was used to explain the material reactivity.

As the corrosion ability of materials depends on various conditions, then, the large number of experimental factors to consider remained the major obstacle for the experimenter to understand the alteration mechanisms. Nowadays, the chemometric approach is considered as powerful tool for studying the corrosion and protection process. Many works introduced the use of experimental designs for understand metals corrosion and inhibition [12]-[18]. Among them, only de Lago *et al.* [19] used the experimental design to study the effect of 2-amino-5-mercapto-1,3,4-thiadiazole (AMT) as inhibitor for bronze protection in artificial rainwater.

However, the experimental design use for studying bronze corrosion, to the best of our knowledge, was not yet investigated.

The aim of the present investigation was to model the experimental conditions of tin bronze patination using full factorial experimental design. The main interests for application of an artificial patina are rebuilding of historical artifacts, works of arts and for the purpose of scientific research.

2. Methodology

2.1. Electrochemical Test

High-purity Cu and Sn metals (Goodfellow copper rod > 99.999 wt. % and Sn Johnson-Matthey tin slug > 99.9985 wt. %) and Cu-10 wt. % Sn alloy (5.60 at. % Sn) were used in this study. The bronze was prepared from the pure copper and tin through a procedure detailed elsewhere [20]. The working electrodes made from this alloy were embedded into a chemically inert resin with an exposed area (only one face) of 0.33 cm^2. Before use, the electrodes were mechanically polished

with abrasive paper up to 2500 SiC grade, washed with distilled water and dried in a room temperature.

The electrochemical experiments were carried out in a standard three-electrode cell, with a large size graphite sheet as counter electrode and a saturated calomel electrode (SCE) as reference electrode. The electrochemical impedance spectroscopy (EIS) measurements were performed with an Autolab® PGSTAT 20 potentiostat equipped with an impedance analysis module. Software NOVA was used for the instrumentation control, data treatment as well as spectra fitting.

The chloride patina was electrochemically formed at the Cu10Sn bronze using potentiodynamic technique (anodic potential sweep) according to the experimental design described here above.

2.2. Experimental Design Approach

The full factorial design was used to study the influence of different experimental factors on the chloride patina formation at the bronze substrate. The patina layer was artificially electrodeposited at the Cu10Sn alloy using potentiodynamic technique. After a preliminary investigation, three experimental variables were chosen:

U_1: first factor representing the immersion time in the chloride electrolyte, t.

U_2: second factor representing the potential limit for the anodic sweep, E_{lim}.

U_3: third factor representing the potential scan rate, v.

Table 1 summarizes the experimental field.

The total number of the experiments to be carried out was 2^n [13]-[19], where n is the number of experimental variables. Therefore, the experimental design consisted of eight experiments.

The experimental design as well as the experimental matrix is listed in Table 2.

The experimental responses studied were the electrochemical parameters obtained after fitting of the the EIS spectra for the different experiments.

- E_{corr}: the corrosion potential, the rest potential at which the EIS spectra were taken.
- Re: the electrolyte resistance,
- R_t: the charge transfer resistance,
- CPE_{dl}: the constant phase element associated to the double layer capacitance,
- k: the effective transfer rate of the chemical reaction (Gerischer type impedance, see below),
- $1/Y_0$: the admittance parameter (Gerischer type impedance, see below).

Table 1. Experimental field.

Factors	U_1 (immersion time) (min)	U_2 (limit potential) (V/SCE)	U_3 (scan rate) ($mV \cdot s^{-1}$)
−1	30	0.1	1
+1	60	1	10

Table 2. Experimental matrix-Experimental design.

Experiment	Experimental design			Experimental matrix		
				t (min)	E_{limi} (V/SCE)	ν (mV·s^{-1})
	X_1	X_2	X_3	U_1	U_2	U_3
1	−1	−1	−1	30	0.1	1
2	1	−1	−1	60	0.1	1
3	−1	1	−1	30	1	1
4	1	1	−1	60	1	1
5	−1	−1	1	30	0.1	10
6	1	−1	1	60	0.1	10
7	−1	1	1	30	1	10
8	1	1	1	60	1	10

The first order-model for the three variables can be represented by the following equation:

$$\psi_i = b_0 + b_1X_1 + b_2X_2 + b_3X_3 + b_{12}X_1X_2 + b_{13}X_1X_3 + b_{23}X_2X_3 + b_{123}X_1X_2X_3 \quad (1)$$

where:

- ψ_i is the experimental response,
- X_i is the coded variable relative to natural variable U_i, which obtained as detailed elsewhere [11],
- b_0 is the intercept,
- b_i represents the main effects of the factor i,
- b_{ij} represents the interaction between the factors i and j,
- b_{ijk} represents the interaction between the factors i, j and k.

The coefficients (b_i, b_{ij} and b_{ijk}) were calculated by the least squares method using [16]:

$$B = \left(X'X\right)^{-1} X'Y \quad (2)$$

where:

- B is the vector of the estimates of the coefficients,
- X is the model matrix,
- X' is the transposed matrix,
- $\left(X'X\right)$ is the information matrix,
- $\left(X'X\right)^{-1}$ is the dispersion matrix,
- Y is the vector of the experimental design.

3. Results and Discussion

3.1. EIS Characterization

EIS analyses of the electrochemically formed interfaces according to the experimental design were performed. In fact, after patina deposition at the bronze substrate according to the experimental design described above, the Nyquist plots of the EIS spectra were recorded for 5 minutes of immersion in 1 g/L Na_2SO_4

electrolyte and the results are shown in Figure 1.

As Figure 1 shows, the Nyquist plots obtained for the different bronze surfaces

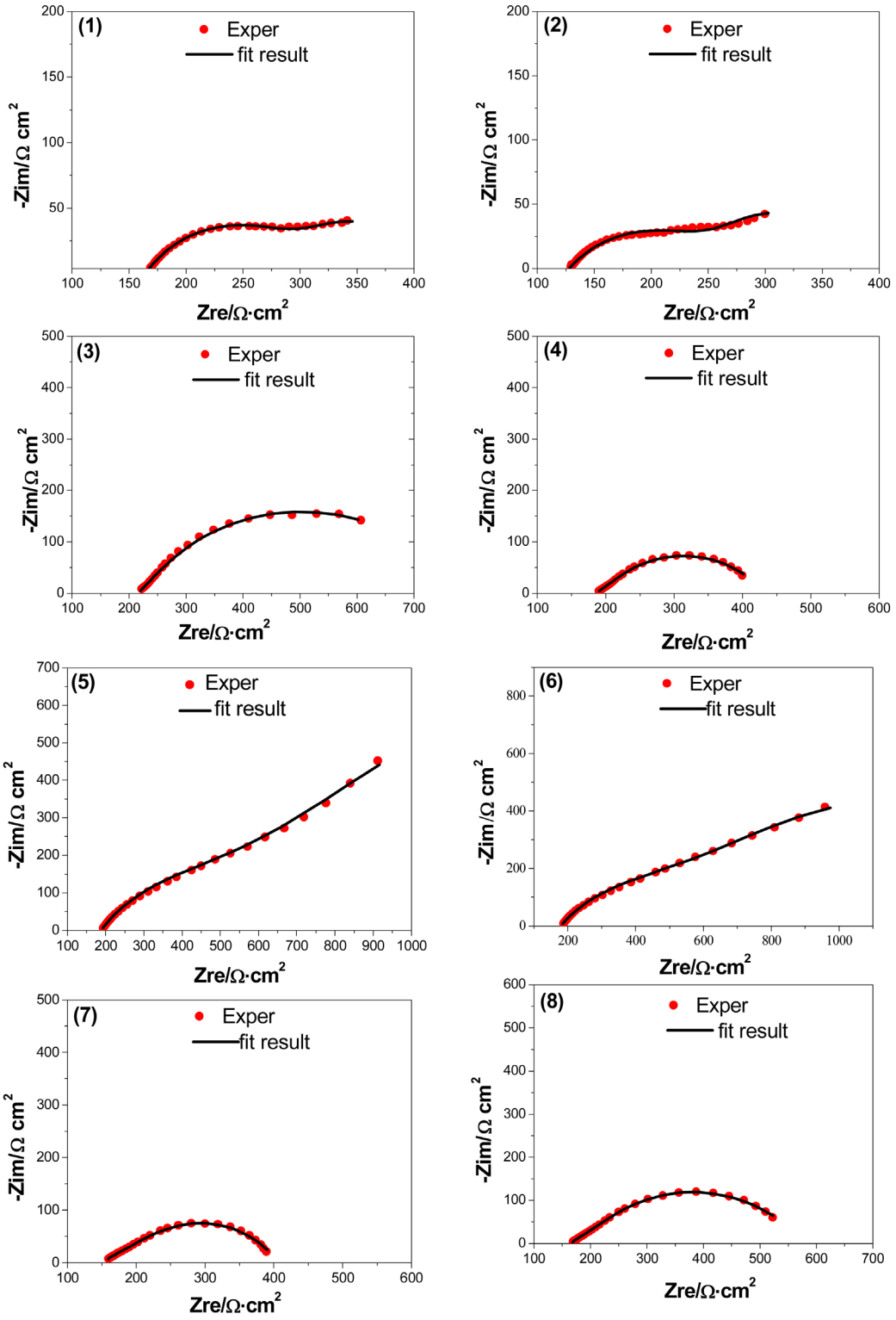

Figure 1. Electrochemical impedance spectra obtained for the patinated bronze immersed in 1 g·L^{-1} Na_2SO_4 solution in different condition.

are characterized by two badly separately capacitive loops. At high frequency, the depressed semi-circle in the high frequency range could be related to the charge transfer process. Moreover, the low frequency tail at near 45^0 could be attributed to mass transfer control of the corrosion process. The EIS spectra were analyzed according to the equivalent circuit presented in **Figure 2**.

The equivalent circuit consists of the electrolyte resistance (R_e), the double layer capacitance (CPE_{dl}) the charge transfer resistance (R_t) and the Gerischer element (G).

Instead of using capacitance in the equivalent circuit, a constant phase element was introduced (CPE_{dl}). It represents the deviation from the true capacitor behavior. The impedance of a constant phase element is defined in Equation (3):

$$Z_{CPE}(\omega) = Y_0^{-1}(j\omega)^{-n} \tag{3}$$

where:

- Y_0 is the admittance representative for the CPE_{dl}.
- n_d is related to the non-equilibrium current distribution due to the surface roughness and defects.

$\mathrm{CPE_{dl}}$ describes a pure inductor for the case $n = -1$, an ideal resistor for $n = 0$ and an ideal capacitance for $n = 1$. In our case, the CPE_{dl} could be related to the non-uniform porous patina layer grown at the bronze surface.

The Gerischer impedance was introduced to describe a diffusion type impedance in which the species also participates in a chemical reaction along the diffusion path [18]. This impedance was generally observed in a mixed conducting solid electrolyte systems [2]. The Gerischer impedance is given by Equation (4) [21]:

$$Z_G(\omega) = \frac{Z_0}{\sqrt{k + j\omega}} \tag{4}$$

where, k holds for the effective transfer rate of the chemical reaction, and the admittance element $Y_0 = 1/Z_0$.

It is interesting to note that the obtained equivalent circuit was different to that found in the literature for bronze corrosion in sulfate containing media. The proposed model consisted of two parallel RC circuits and three parallel RC circuits [22] [23].

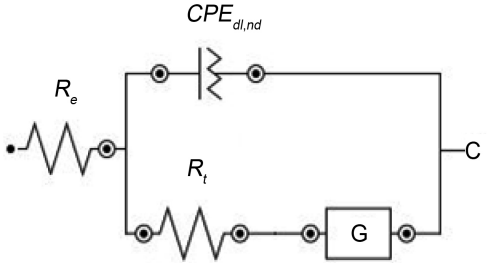

Figure 2. The equivalent electrical circuits used for fitting of the impedance spectra.

3.2. Experimental Design Study

From the EIS spectra depicted in Figure 1, the best fitting parameters corresponding to the equivalent circuit presented in Figure 2 were extracted. The results are summarized in Table 3.

The responses were analyzed by regression analysis according to the proposed mathematical model. The estimated coefficients models parameters were listed in Figure 3.

In order to evaluate the weight of the different coefficients on the electrochemical parameters Pareto analysis was performed [24]. Plots of the contribution of each term are displayed in Figure 3 where the percentage effect P_i of every term i, was calculated through Equation (5):

$$P_i = 100\left(\frac{b_i^2}{\sum_i b_i^2}\right) \tag{5}$$

Analysis of the statistical results showed that:

- The factors b_3, b_2 and b_{23} could explain about 96% of the corrosion potential variation
- The scan rate is the most influent parameter as P_3 = 48%.
- The third factor was the most significant factor for the electrolyte resistance variation as P_3 = 57.2%.
- b_3, b_{123} and b_2 were the most significant for charge transfer resistance evolution. The main effect was attributed to the limit potential P_2 = 54.1%.
- b_3, b_{12} and b_{123} could contribute to 93.1% of the double layer capacitance. The third factor was the most important (P_3 = 40.7%).
- 92.4% of the depressed feature coefficient variation was due to b_3, b_{12} and b_{123}, the main effect was linked to the interaction between the second and third factor (P_{23} = 45.8%).
- The limit potential could present the main effect on the admittance parameter responses $1/Y_0$, P_2 = 34%.
- The second factor was the most important parameter for the effective transfer rate of the chemical reaction as P_2 = 66.8%.

Table 3. Experimental responses extracted from the EIS spectra.

Experiment	E_{corr} (SCE/V)	R_e ($\Omega\cdot cm^2$)	R_t ($\Omega\cdot cm^2$)	n	CPE_{dl} (μF)	$1/Y_0$	$1/k$ (s)
1	−0.031	163.02	104.94	0.52	32.89	95.2	12.5
2	−0.030	125.73	221.76	0.46	70.32	62.5	25
3	−0.020	211.2	190.41	0.59	72.74	3086.4	0.32
4	−0.035	185.13	124.08	0.60	41.7	1626	1.01
5	−0.087	164.67	30.063	0.61	14.00	1968	20
6	−0.088	153.45	82.17	0.61	10.98	2061.8	5
7	−0.043	152.79	69.63	0.61	21.28	1636.6	0.13
8	−0.035	164.01	81.51	0.55	13.00	2433.0	0.22

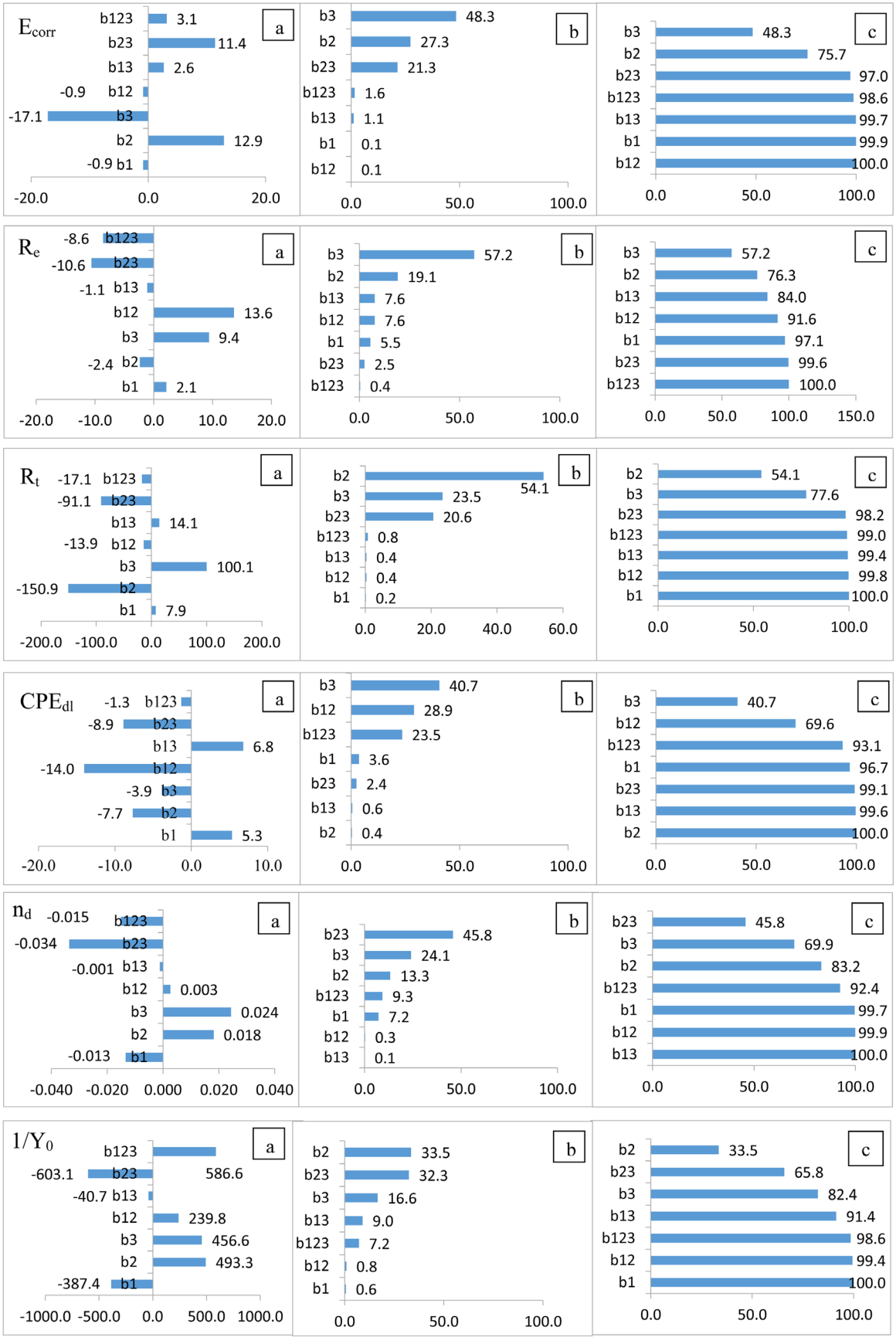
Ecorr
b123 3.1
b23 11.4
b13 2.6
-0.9 b12
-17.1 b3
b2 12.9
-0.9 b1
-20.0 0.0 20.0
a
b3 48.3
b2 27.3
b23 21.3
b123 1.6
b13 1.1
b1 0.1
b12 0.1
0.0 50.0 100.0
b
b3 48.3
b2 75.7
b23 97.0
b123 98.6
b13 99.7
b1 99.9
b12 100.0
0.0 50.0 100.0
c
Re
-8.6 b123
-10.6 b23
-1.1 b13
b12 13.6
b3 9.4
-2.4 b2
b1 2.1
-20.0 -10.0 0.0 10.0 20.0
a
b3 57.2
b2 19.1
b13 7.6
b12 7.6
b1 5.5
b23 2.5
b123 0.4
0.0 50.0 100.0
b
b3 57.2
b2 76.3
b13 84.0
b12 91.6
b1 97.1
b23 99.6
b123 100.0
0.0 50.0 100.0 150.0
c
Rt
-17.1 b123
-91.1 b23
b13 14.1
-13.9 b12
b3 100.1
-150.9 b2
b1 7.9
-200.0 -100.0 0.0 100.0 200.0
a
b2 54.1
b3 23.5
b23 20.6
b123 0.8
b13 0.4
b12 0.4
b1 0.2
0.0 20.0 40.0 60.0
b
b2 54.1
b3 77.6
b23 98.2
b123 99.0
b13 99.4
b12 99.8
b1 100.0
0.0 50.0 100.0
c
CPEdl
-1.3 b123
-8.9 b23
b13 6.8
-14.0 b12
-3.9 b3
-7.7 b2
b1 5.3
-20.0 -10.0 0.0 10.0
a
b3 40.7
b12 28.9
b123 23.5
b1 3.6
b23 2.4
b13 0.6
b2 0.4
0.0 50.0 100.0
b
b3 40.7
b12 69.6
b123 93.1
b1 96.7
b23 99.1
b13 99.6
b2 100.0
0.0 50.0 100.0
c
nd
-0.015 b123
-0.034 b23
-0.001 b13
b12 0.003
b3 0.024
b2 0.018
-0.013 b1
-0.040 -0.020 0.000 0.020 0.040
a
b23 45.8
b3 24.1
b2 13.3
b123 9.3
b1 7.2
b12 0.3
b13 0.1
0.0 50.0 100.0
b
b23 45.8
b3 69.9
b2 83.2
b123 92.4
b1 99.7
b12 99.9
b13 100.0
0.0 50.0 100.0
c
1/Y0
b123
-603.1 b23 586.6
-40.7 b13
b12 239.8
b3 456.6
b2 493.3
-387.4 b1
-1000.0 -500.0 0.0 500.0 1000.0
a
b2 33.5
b23 32.3
b3 16.6
b13 9.0
b123 7.2
b12 0.8
b1 0.6
0.0 50.0 100.0
b
b2 33.5
b23 65.8
b3 82.4
b13 91.4
b123 98.6
b12 99.4
b1 100.0
0.0 50.0 100.0
c

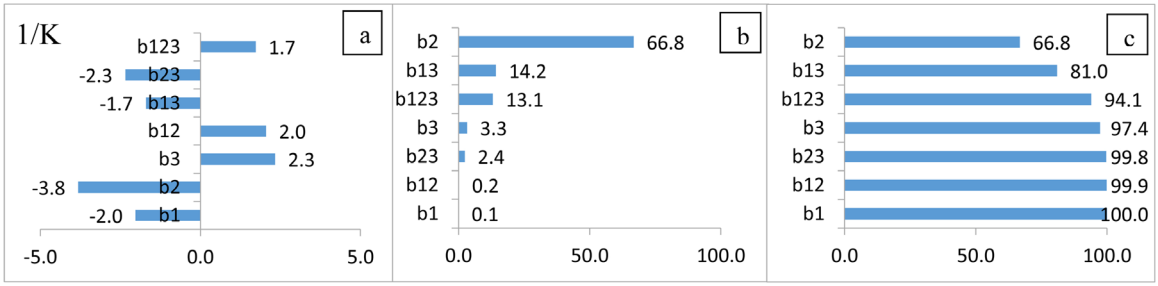

Figure 3. Pareto analysis for the experimental responses (a) The estimated model coefficients, (b) Pareto charts and (c) cumulative Pareto charts for the different electrochemical responses.

It could be concluded from the previous results that the scan rate was the most important factor for the response E_{corr}, R_e and CPE_{dl}. This parameter could reflect the kinetic of the patina growth at the Cu10Sn alloy.

For Y_0, R_t and k, we found that the limit potential of anodic polarization curve was the most important. Such a result could be related to the composition and the structure of the chloride patina.

Finally, the interaction between the scan rate and the limit potential was the important factor for n variation. Therefore this parameter could affect the to the non-equilibrium current distribution linked to the surface roughness and patina porosity.

4. Conclusions

The aim of the present work was to study the corrosion behavior of chloride patinated bronze in 1 g/l Na_2SO_4 electrolyte using EIS technique. A full factorial design was chosen to study the effect of the immersion time, the limit potential and the scan rate on the patina growth at the bronze substrate. The experimental responses were the electrochemical parameters obtained after fitting the EIS spectra. We found that the most suitable equivalent circuit to describe the electrochemical behavior of patinated bronze is a Randles type containing an additional Gerischer impedance element. When analyzing the experimental responses, we found that the scan rate was the most influent factor for E_{corr}, R_e and CPE_{dl} variation. However, the limit potential was the significant factor for R_t, Y_0 and k variation.

We hope to investigate the effects of plant extracts on the corrosion of bronze covered with chloride patina by potentiodynamic polarization measurement, electrochemical impedance spectroscopy and SEM/EDX methods.

References

[1] Robbiola, L. and Portier, R.J. (2006) A Global Approach to the Authentication of Ancient Bronzes Based on the Characterization of the Alloy-Patina-Environment System. *Journal of Cultural Heritage*, **7**, 1-12. https://doi.org/10.1016/j.culher.2005.11.001

[2] Alberghina, M.F., Barraco, R., Brai, M., Schillaci, T. and Tranchina, T. (2011) Integrated Analytical Methodologies for the Study of Corrosion Processes in Archaeo-

logical Bronzes. *Spectrochimica acta Part B: Atomic Spectroscopy*, **66**, 129-137. https://doi.org/10.1016/j.sab.2010.12.010

[3] Ingo, G., Angelini, E., Bultrini, G., Calliari I., Dabala, M. and De Caro, T. (2002) Study of Long-Term Corrosion Layers Grown on High-Tin Leaded Bronzes by Means of the Combined Use of GDOES and SEM+ EDS. *Surface and Interface Analysis*, **34**, 337-342. https://doi.org/10.1002/sia.1312

[4] Muresan, L., Varvara, S., Stupnišek-Lisac, E., Otmačić, H., Marušić, K., Horvat-Kurbegović, S., Robbiola, L., Rahmouni. K. and Takenouti, H. (2007) Protection of Bronze Covered with Patina by Innoxious Organic Substances. *Electrochimica Acta*, **52**, 7770-7779. https://doi.org/10.1016/j.electacta.2007.02.024

[5] Robbiola, L., Tran, T.T.M., Dubot, P., Majerus, O. and Rahmouni, K. (2008) Characterisation of Anodic Layers on Cu-10Sn Bronze (RDE) in Aerated NaCl Solution. *Corrosion Science*, **50**, 2205-2215. https://doi.org/10.1016/j.corsci.2008.06.003

[6] Marušić, K., Otmačić, H., Horvat-Kurbegović, Š., Takenouti, H. and Stupnišek-Lisac, E. (2009) Comparative Studies of Chemical and Electrochemical Preparation of Artificial Bronze Patinas and Their Protection by Corrosion Inhibitor. *Electrochimica Acta*, **54**, 7106-7113. https://doi.org/10.1016/j.electacta.2009.07.014

[7] Kosec, T., Ćurković, H.O. and Legat, A. (2010) Investigation of the Corrosion Protection of Chemically and Electrochemically Formed Patinas on Recent Bronze. *Electrochimica Acta*, **56**, 722-731. https://doi.org/10.1016/j.electacta.2010.09.093

[8] Liao, X.N., Cao, F.H., Chen, A.N., Liu, W.J., Zhang, J.Q. and Cao, C.-N. (2012) *In-Situ* Investigation of Atmospheric Corrosion Behavior of Bronze under Thin Electrolyte Layers Using Electrochemical Technique. *Transactions of Nonferrous Metals Society of China*, **22**, 1239-1249. https://doi.org/10.1016/S1003-6326(11)61311-3

[9] Robbiola, L, Blengino, J.M. and Fiaud, C. (1998) Morphology and Mechanisms of Formation of Natural Patinas on Archaeological Cu-Sn Alloys. *Corrosion Science*, **40**, 2083-2111. https://doi.org/10.1016/S0010-938X(98)00096-1

[10] Souissi, N., Sidot, E., Bousselmi, L., Triki, E. and Robbiola, L. (2007) Corrosion Behaviour of Cu-10Sn Bronze in Aerated NaCl Aqueous Media—Electrochemical investigation. *Corrosion Science*, **49**, 3333-3347. https://doi.org/10.1016/j.corsci.2007.01.013

[11] Aouadi, S. and Souissi, N. (2016) Early Stages of Tin Bronze Corrosion in Neutral Aqueous Chloride Media: Electrochemical and FTIR Investigations. *Materials and Corrosion*, **67**, 1105-1113. https://doi.org/10.1002/maco.201608856

[12] Hajeeh, M. (2003) Estimating Corrosion: A Statistical Approach. *Materials & Design*, **24**, 509-518.

[13] Rios, E.C., Zimer, A.M., Mendes, P.C.D., Freitas, M.B.J., de Castro, E.V.R., Mascaro, L.H. and Pereira, E.C. (2015) Corrosion of AISI 1020 Steel in Crude Oil Studied by the Electrochemical Noise Measurements. *Fuel*, **150**, 325-333.

[14] Luciano, G., Traverso, P. and Letardi, P. (2010) Applications of Chemometric Tools in Corrosion Studies. *Corrosion Science*, **52**, 2750-2757.

[15] Rajahram, S.S., Harvey, T.J. and Wood, R.J.K. (2010) Full Factorial Investigation on the Erosion-Corrosion Resistance of UNS S31603. *Tribology International*, **43**, 2072-2083.

[16] Souissi, N. and Triki, E. (2008) Modelling of Phosphate Inhibition of Copper Corrosion in Aqueous Chloride and Sulphate Media. *Corrosion Science*, **50**, 231-241.

[17] Mondel, D., Das, S. and Prasad, B. (1998) Study of Erosive-Corrosive Wear Characteristics of an Aluminium Alloy Composite through Factorial Design of Experiments.

Wear, **217**, 1-6.

[18] Forsal, I., Touhami, M.E., Mernari, B., Hajri, J.E. and Baba, M.F. (2006) Use of Experimental Designs to Evaluate the Influence of 2-Mercaptobenzimidazole on the Corrosion of Mild Steel in HCl (1 M) Environment in the Presence of Alcohol Ethoxylate. *Portugaliae Electrochimica Acta*, **28**, 203-212. https://doi.org/10.4152/pea.201003203

[19] De Oliveira, F.J.R., Lago, D.C.B., Senna, L.F., de Miranda, L.R.M. and D'elia, E. (2009) Study of Patina Formation on Bronze Specimens. *Materials Chemistry and Physics*, **115**, 761-770.

[20] Sidot, E., Souissi, N., Bousselmi, L., Triki, E. and Robbiola, L. (2006) Study of the Corrosion Behaviour of Cu-10Sn Bronze in Aerated Na2SO4 Aqueous Solution. *Corrosion Science*, **48**, 2241-2257.

[21] Boukamp, B.A. and Bouwmeester, H.J.M. (2003) Interpretation of the Gerischer Impedance in Solid-State Ionics. *Solid State Ionics*, **157**, 29-33.

[22] Boukamp, B.A. (2004) Electrochemical Impedance Spectroscopy in Solid-State Ionics: Recent Advances. *Solid State Ionics*, **169**, 65-73.

[23] Boukamp, B.A., Raming, T.P., Winnubst, A.J.A. and Verweij, H. (2003) Electrochemical Characterisation of 3Y-TZP-Fe2O3 Composites. *Solid State Ionics*, **158**, 381-394.

[24] Haaland, P.D. (1989) Experimental Design in Biotechnology. Marcel Dekker, New York.